

Robustness analysis in forward modelling gravity data in crustal/lithospheric studies

Vladimír POHÁNKA¹, Peter VAJDA¹, Miroslav BIELIK^{1,2},
Jana DÉREROVÁ¹

¹ Geophysical Institute of the Slovak Academy of Sciences
Dúbravská cesta 9, 845 28 Bratislava, Slovak Republic; e-mail: geofpohv@savba.sk;
geofvajd@savba.sk; geofmiro@savba.sk; geofjade@savba.sk

² Department of Applied and Environmental Geophysics, Faculty of Natural Sciences,
Comenius University, Mlynská dolina, pav. G, 842 48 Bratislava, Slovak Republic
e-mail: bielik@fns.uniba.sk

Abstract: The robustness of the gravimetric forward modelling is investigated by applying the harmonic inversion procedure at the input which is the difference of the calculated and measured surface gravity. The gravity data are taken from two profiles in the Carpathian-Pannonian Basin region. The result of the inversion are density models obtained from the original two-layer models with various horizontal boundary depth and density contrast. The deformation of the originally planar boundary is the measure of the mismatch between calculated and measured data. The calculated deformation has reached up to tens of kilometers and thus the uncertainties in determining the geometry of disturbing bodies by the forward modelling are substantial.

Key words: inverse problem, forward gravity modelling, harmonic inversion method

1. Introduction

As it is well known, the gravimetric inverse problem has infinitely many solutions, and thus it is an ill-posed problem. This means that a small change of the gravity data (which represent the input) can result in a very large change (of the parameters) of the solution. If the inverse problem is solved using some parametrization and linearization, this ill-posedness implies that before the numerical solution there must be applied some regularization. Alternatively, the inverse problem is solved by the iterative

forward modelling: this requires a fair starting model and a suite of additional constraining information that comes from other geophysical, or more generally, geoscientific disciplines. In any case, the solution that is found represents only one possible solution from the infinite set of all solutions. Moreover, the data are always given with some errors and there remains a substantial uncertainty (of the parameters) of the solution which grows with the depth from the earth's surface.

There is also another source of uncertainty by solving the gravimetric inverse problem using the forward modelling methods: the model of the density distribution is considered as the resulting model when the match (fit) between the calculated and the observed gravity data is sufficiently good. There remains the question what does it exactly mean: thus whether there is an exact measure of the difference between the calculated and the observed gravity data or the suitability of the resulting model is determined by the interpretator.

Here we investigate the robustness of the gravimetric forward modelling by considering the influence of the difference between the calculated and the observed gravity data on the parameters of the resulting model. This difference is considered as the input for the solution of the inverse problem by the harmonic inversion method (see *Pohánka, 2003*), developed and tested at the Geophysical Institute of the Slovak Academy of Sciences. We have to emphasize that the now available version of the harmonic inversion method works only for the planar surface of the Earth, thus the gravity inversion is performed under this assumption (which does not alter our conclusions). We do not perform the general gravity inversion (which is the main task of the harmonic inversion), but only the partial one: we calculate the vertical deformation of the (originally planar) contact surface between two layers with different density (caused by the non-zero surface gravity input); as it is well known, the exactly horizontal density contrast does not have any effect on the surface gravity. The case of a density contrast surfaces is interesting because such surfaces are assumed within the earth crust or lithosphere, or between lithosphere and asthenosphere. The deformation of this originally planar contact surface then represents the measure of the quality of the density model calculated by the forward modelling method. We perform our analysis for contact surfaces of several reasonable density contrast values at several depths within the lithosphere.

2. Data

Profiles 5 and 8 are two of nine geotranssects (Fig. 1) that have been modelled using the 2-D integrated geophysical modelling method in order to study the lithospheric structure and to create a new map of lithospheric thicknesses for the Carpathian-Pannonian Basin region. Integrated lithospheric geophysical modelling combines the interpretation of surface heat flow, geoid, gravity, and topography data for the determination of the lithospheric thermal structure.

The program used consists of a 2-D finite element algorithm to calculate the temperature distribution based on a user-defined lithospheric structure where each body is characterized by its density, thermal conductivity and heat production. The body structure is as much as possible constrained by

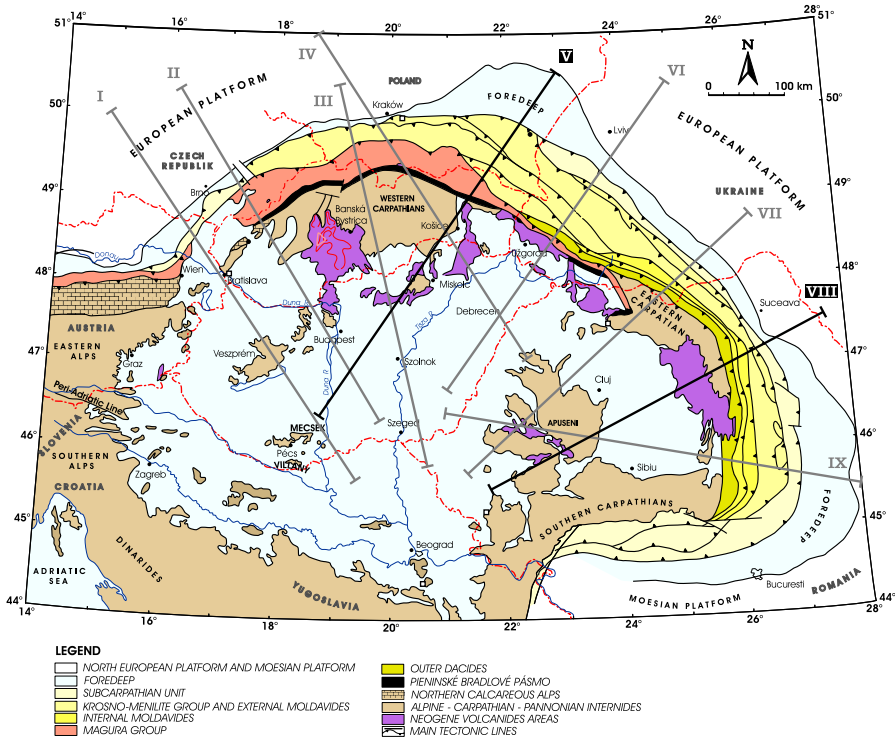


Fig. 1. Schematic tectonic map of the Carpathian-Pannonian region with studied profiles.

existing seismic and geological data. After the calculation of the temperature distribution, the body densities are modified at each node of the finite element grid taking into account the thermal expansion coefficient. With this modified density distribution, we calculate the gravity and geoid variations and the topography, after having calculated the average lithospheric density for every column of the grid. Since geoid, gravity, and topography data have all different distance dependence on density variations data, they serve as constraints for lateral temperature variations. Data and model results are compared and the model is then changed interactively by trial and error until an acceptable fit is obtained. Detailed description of method can be found in *Zeyen and Fernández (1994)* and *Dérerová et al. (2006)*.

We used free air gravity anomalies in our modelling (Fig. 2). They were taken from the TOPEX 1-min gravity data set (<ftp://topex.ucsd.edu/pub>, *Sandwell and Smith, 1997*). For the different transects we extracted the data from the mentioned data set along a strip 50 km to each side of the transects in order to have some measure of the 3-D variability of the input data. These data (and the modelled lithospheric structures) for profiles 5

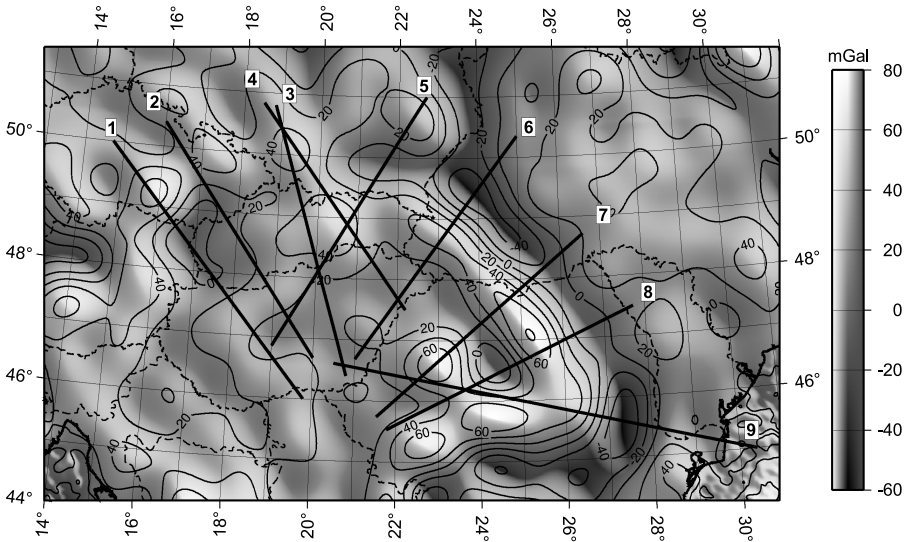


Fig. 2. Smoothed free-air gravity anomaly map of the Carpathian-Pannonian Basin region (from TOPEX gravity data, 1 min grid, <ftp://topex.ucsd.edu/pub>, contour interval 10 mGal) with studied profiles.

and 8 are shown in Fig. 3 as dots with uncertainty bars which indicate the 1σ deviation within the mentioned strip. Full results and a new map of lithospheric thickness obtained by this method can be found in Zeyen *et al.* (2002) and D ererova *et al.* (2006).

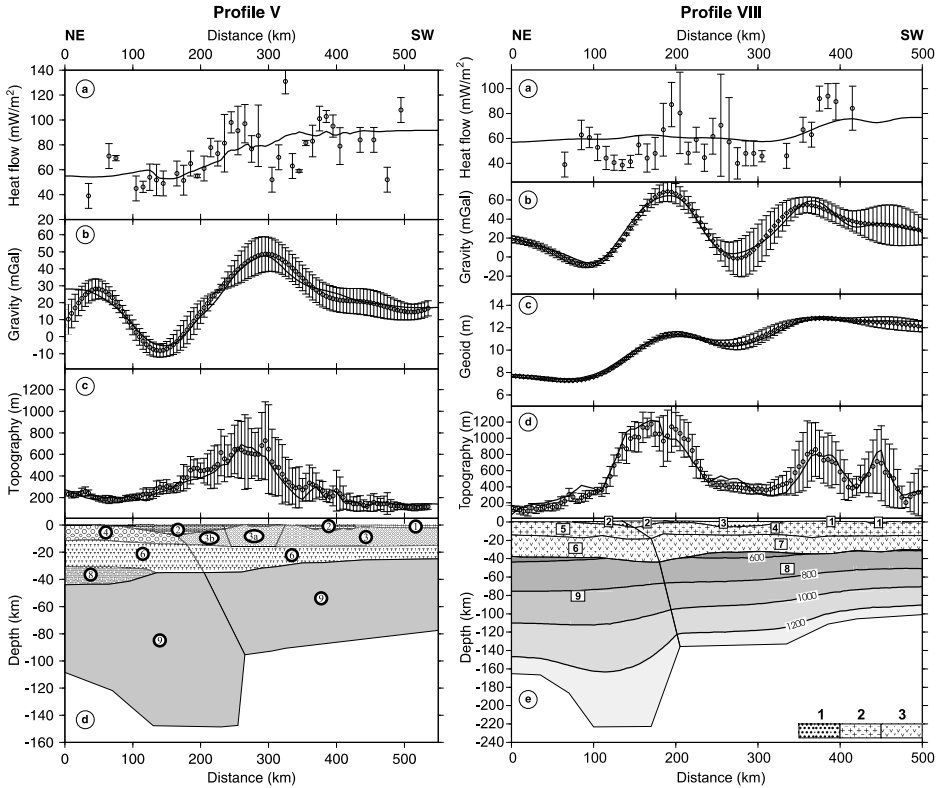


Fig. 3. Lithospheric models for profiles 5 and 8 with surface heat flow, free-air gravity anomaly, geoid (only profile 8) and topography with dots corresponding to measured data with uncertainty bars and solid lines to calculated values. Keys: Profile 5 (1 Neogene sediments, 2 flysch and volcanics, 3 Carpathian and Pannonian upper crust, 3a Inner Western Carpathian upper crust, 3b Central Western Carpathian upper crust, 4 European upper crust, 6 European lower crust, 8 high density lower crust, 9 lower mantle lithosphere). Profile 8 (1 Neogene sediments, 2 flysch, foreland basin, sedimentary cover of European Platform, 3 volcanics, 4 Carpathian and Pannonian upper crust, 5 European Platform upper crust, 6 European Platform lower crust, 7 Carpathian and Pannonian lower crust, 8 Carpathian and Pannonian mantle lithosphere, 9 European mantle lithosphere). In the lithospheric mantle, isotherms are indicated at every 200 °C.

3. Method

For each of the above mentioned profiles 5 and 8, the input for the gravity inversion was the difference of the calculated and measured surface gravity at the profile. This difference was considered as if it were a measured value of gravity at the surface of the Earth; the surface was treated as planar.

As the harmonic inversion method needs for the calculation of the 3-dimensional density distribution the given 2-dimensional surface gravity data, it was first necessary to calculate the surface gravity at certain rectangle at the Earth surface (containing the points at the profile). This was accomplished by the interpolation method developed by one of the authors (Pohánka, 2005); this method allows to interpolate (and extrapolate) to a smooth function at the whole surface (even if the input data points lie at a single line).

The harmonic inversion method in its latest version (see Pohánka, 2003p, 2004) calculates the solution of the inverse problem in two steps:

1. First, the so-called information function is calculated from the given surface gravity data; these data should be given in a rectangle at the surface, called hereafter the surface domain.

The information function is defined as a maximally smooth function having the extrema-conserving property and depending linearly on the surface gravitation. The maximal smoothness is defined by the requirement that the information function is a n -harmonic function (in the halfspace below the surface) for certain small integer n .

The extrema-conserving property means that for the surface gravitational field of a point source (lying below the surface), the information function has its main extremum exactly at the point source.

The name “information function” reflects the fact that this function allows to obtain the 3-dimensional information about the subsurface distribution of sources of the gravity field from the 2-dimensional surface gravity field (this is a consequence of the extrema-conserving property).

If we choose the information function to be a 3-harmonic function, it is then uniquely (up to a multiplicative factor) determined by the above presented conditions in the form

$$q(x, y, z) = T(x, y, z) a(*, *), \tag{1}$$

where the integral operator $T(x, y, z)$ (acting on the function $a(x, y)$; the asterisks denote dummy variables) is equal to 0 for $z \geq 0$, while for $z < 0$ it is defined as

$$T(x, y, z) f(*, *) = 8 \int_0^\infty du \frac{u^2 z^3}{(u^2 + z^2)^{5/2}} \partial_u \bar{f}(x, y, u), \quad (2)$$

where

$$\bar{f}(x, y, u) = \frac{1}{2\pi} \int_0^{2\pi} d\varphi f(x + u \cos \varphi, y + u \sin \varphi) \quad (3)$$

(thus the function $\bar{f}(x, y, u)$ is the mean value of the function $f(x, y)$ at the circle with origin at the point x, y and radius u). The above defined information function has the same dimension as the surface gravitation and, therefore, it will be called the quasigravitation. The quasigravitation is normalized in such a way that for a single point source the local extrema of the surface gravitation and quasigravitation have the same value.

2. Second, a suitable 3-dimensional domain which is chosen contains the points at which we want to calculate the values of density; this domain is called hereafter the calculation domain. This domain has the form of a rectangular prism whose upper side lies at the (planar) surface of the Earth and which is a part of the surface domain (containing the input data). The reliability of the solution of the inverse problem requires that the surface domain is sufficiently larger than the upper side of the calculation domain and that the depth of the lower side of the calculation domain is sufficiently smaller than the horizontal dimensions of the calculation domain. The calculation domain is divided into a huge number of elementary rectangular domains; within each of these elementary domains the density is assumed to be constant.

The solution of the inverse problem is represented as a set of density values for all elementary domains. This solution is obtained in the iterative way using the already determined information function (for details, see *Pohánka, 2003*). The calculation of the solution requires the definition of a suitable starting model: this model usually comprises several horizontal layers with constant density within each layer, and some number of seeds represented by elementary domains with predefined density values. These seeds are located at the points

of local extrema of the information function. As mentioned above, in our case there were no seeds and only two horizontal layers.

The algorithm of the harmonic inversion aims to find such a solution that the number of different density values is as small as possible (in any case substantially smaller than the number of elementary domains). In fact, all density values are defined already in the starting model. Further, the algorithm aims to change the density values of elementary domains in such a way that the form of domains containing all elementary domains with certain value of density is as simple as possible. In other words, for each density value, the domains with this density value are as compact as possible. This property of the algorithm expresses the aim to obtain the maximally simple particular solution of the inverse problem.

4. Numerical calculation and results

The calculation of the solution of the inverse problem was performed for the regions around profiles 5 and 8 with the calculation parameters presented in Table 1. The interpolated surface gravity (the input of the inversion procedure) and the quasigravitation in the vertical section along the two profiles are presented in Figs. 4 and 8.

The starting model for the solution of the inverse problem was chosen in the form of two horizontal layers, one between the surface and the boundary at certain depth, the other below this boundary. The reason for this choice is that we do not calculate any real density model for the regions of the two profiles, but we need to have some measure of the effect of the nonzero surface gravity mismatch: this measure is expressed as the degree of deformation of the originally planar horizontal boundary.

The density in the upper layer was chosen to be 2680 kg m^{-3} , the density in the lower layer acquired three values: 2780 kg m^{-3} , 2880 kg m^{-3} , 3080 kg m^{-3} (thus the difference density was 100 kg m^{-3} , 200 kg m^{-3} and 400 kg m^{-3} , respectively). The depth of the dividing boundary was chosen to acquire three values: 10 km, 20 km, 30 km. The calculated density distribution in the vertical section along the profiles is presented in Figs. 5, 6, 7 (profile 5) and Figs. 9, 10, 11 (profile 8).

Table 1. Calculation parameters

Parameters	Profile 5	Profile 8
Number of data points at the profile	108	101
Step (km)	5	5
Minimal and maximal gravity values at the profile (mGal)	–10.160 21.070	–22.940 24.370
Mean gravity value (mGal)	0.385	0.216
Dimensions of the surface domain (km)	640 × 240	600 × 240
Step (km)	1	1
Number of data points at the surface	154481	144841
Minimal and maximal gravity values at the surface (mGal)	–10.217 40.266	–22.938 41.951
Mean gravity value (mGal)	2.530	1.546
Horizontal dimensions and depth of the calculation domain (km)	600 × 200 50	560 × 200 50
Step (km)	1	1
Number of elementary domains	6040050	5638050
Minimal and maximal quasigravity values (mGal)	–15.646 41.747	–28.188 45.861
Mean quasigravity value (mGal)	0.616	0.333

5. Discussion and conclusions

Our robustness analysis has revealed that for realistic density contrasts (100, 200 and 400 kg m⁻³) of density interfaces within the crust or lithosphere at depth 10, 20 and 30 km, the uncertainties in determining the geometry of these structural contact surfaces from gravimetric forward modelling (in the absence of additional geoscientific constraints) are substantial. The deformation of the originally planar horizontal contact surface can be of the order of kilometers to tens of kilometers. As expected, the deformation grows significantly with increasing depth of the boundary and with decreasing density contrast.

When the fit was declared between the modelled and the observed grav-

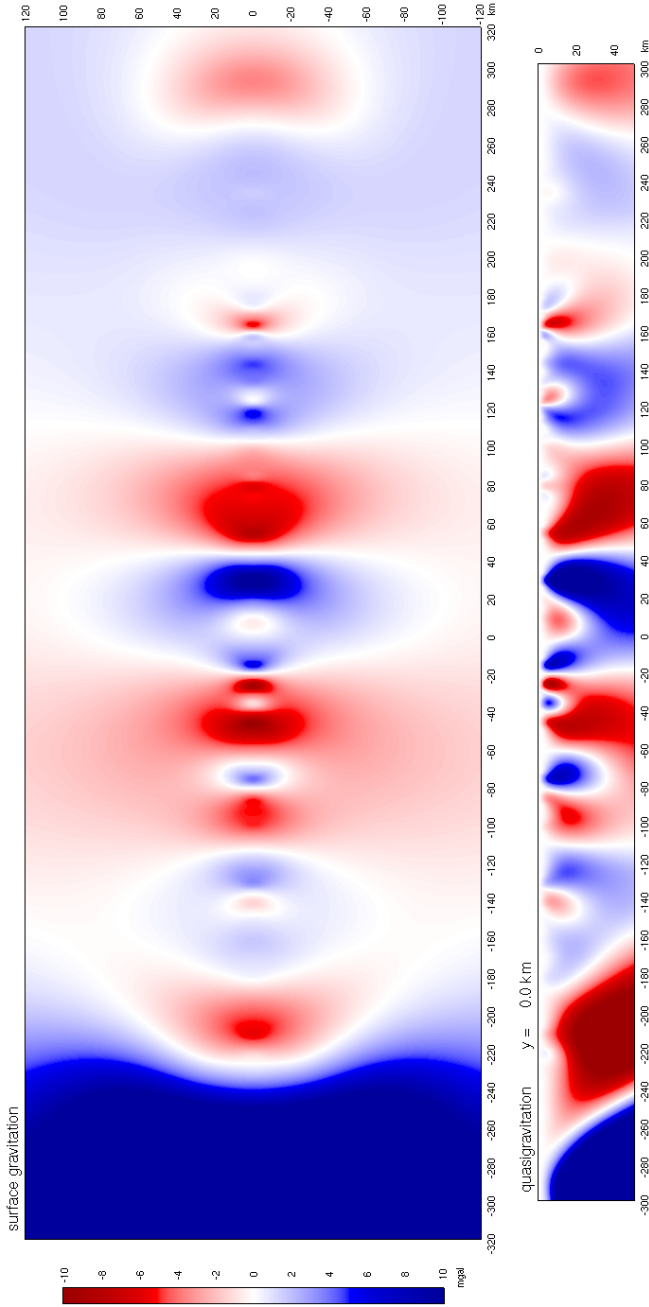


Fig. 4. Profile 5: interpolated surface gravity in the rectangle 640×240 km (top), quasigravitation in the vertical section 600×50 km along the profile (bottom).

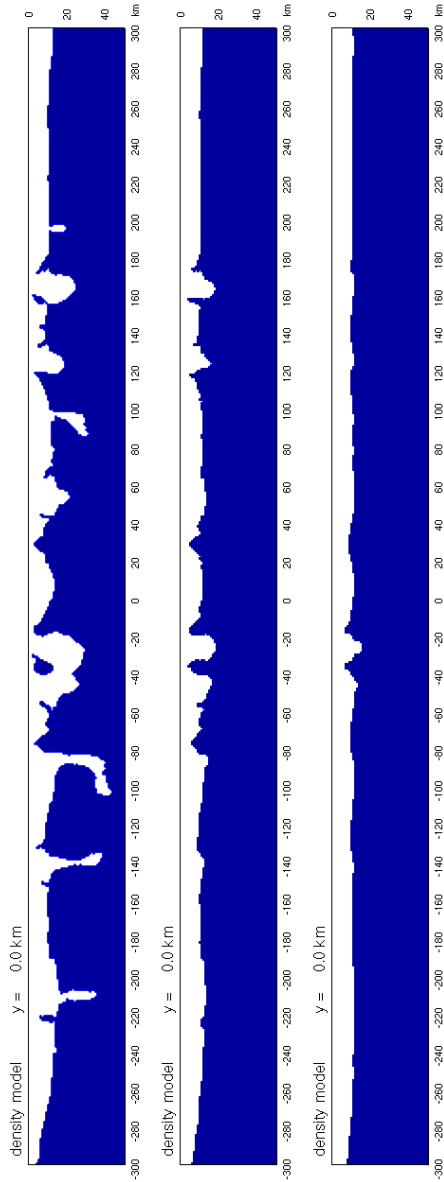


Fig. 5. Profile of density distribution in the vertical section 600×50 km along the profile for the original boundary depth 10 km for difference densities 100, 200 and 400 kg m^{-3} (top to bottom).

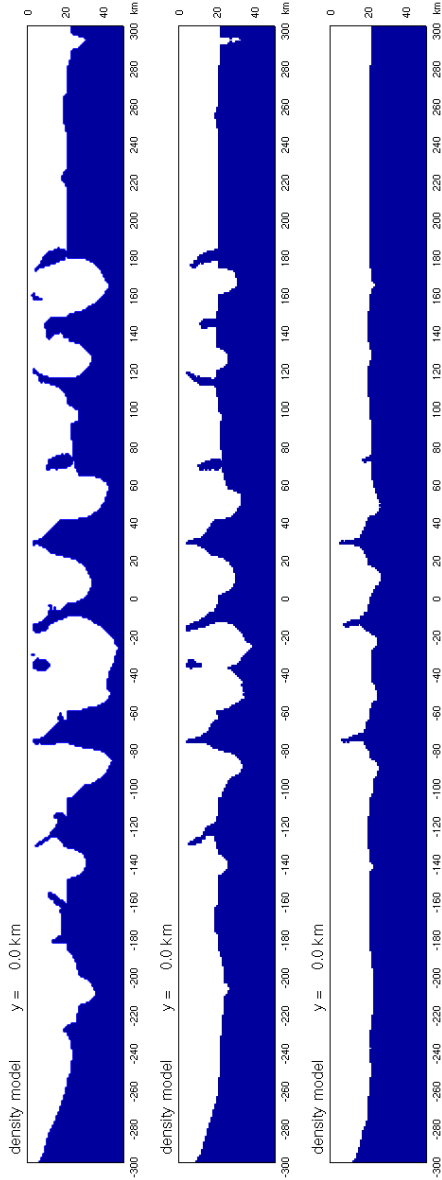


Fig. 6. Profile 5: density distribution in the vertical section 600×50 km along the profile for the original boundary depth 20 km for difference densities 100, 200 and 400 kg m^{-3} (top to bottom).

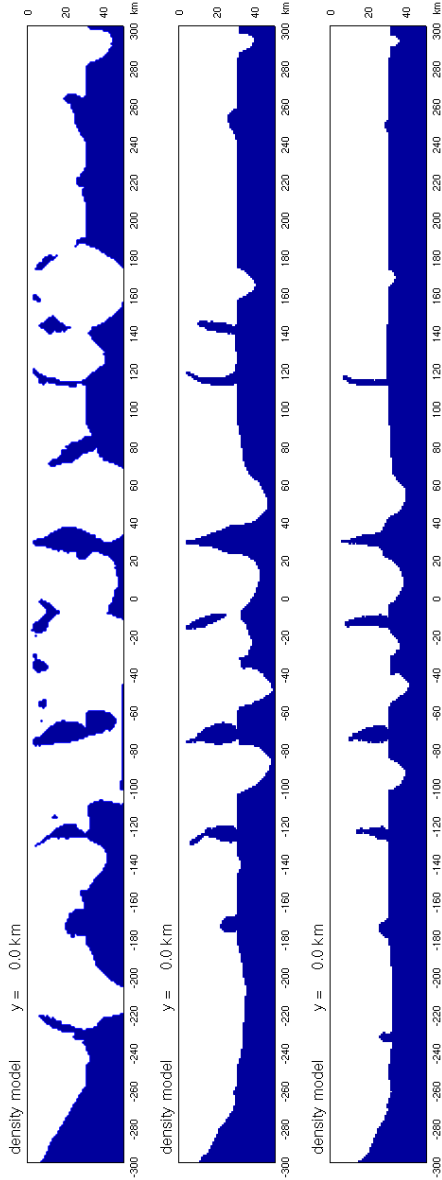


Fig. 7. Profile 5: density distribution in the vertical section 600×50 km along the profile for the original boundary depth 30 km for difference densities 100, 200 and 400 kg m^{-3} (top to bottom).

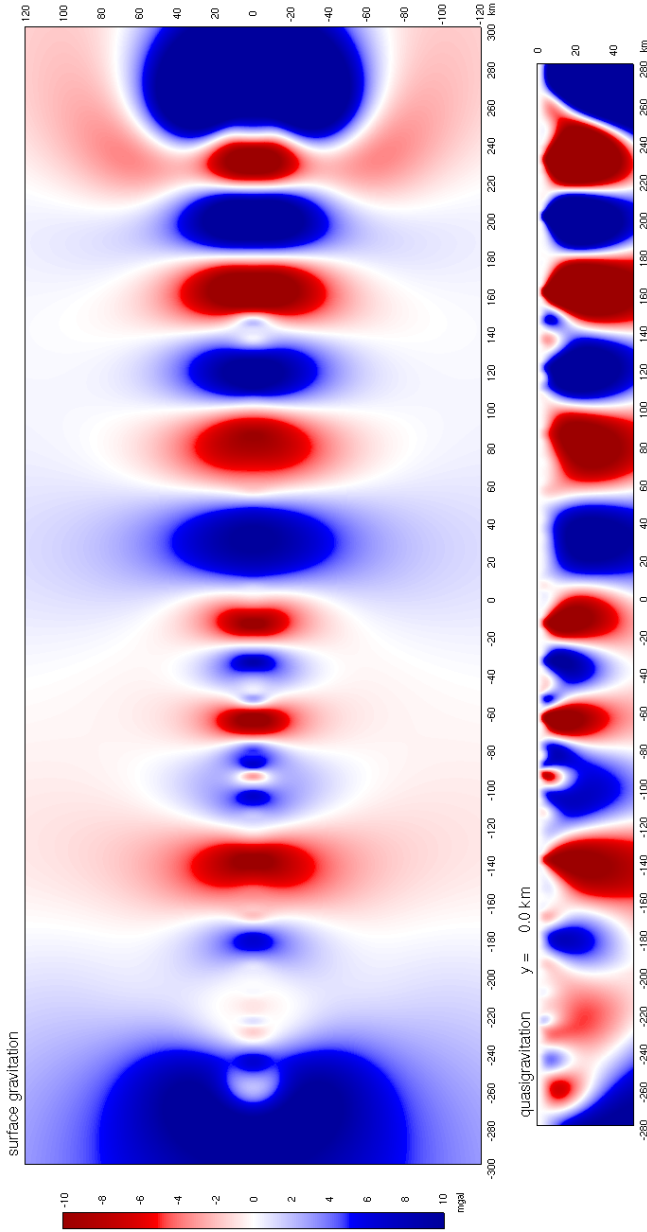


Fig. 8. Profile 8: interpolated surface gravity in the rectangle 600×240 km (top), quasigravitation in the vertical section 560×50 km along the profile (bottom).

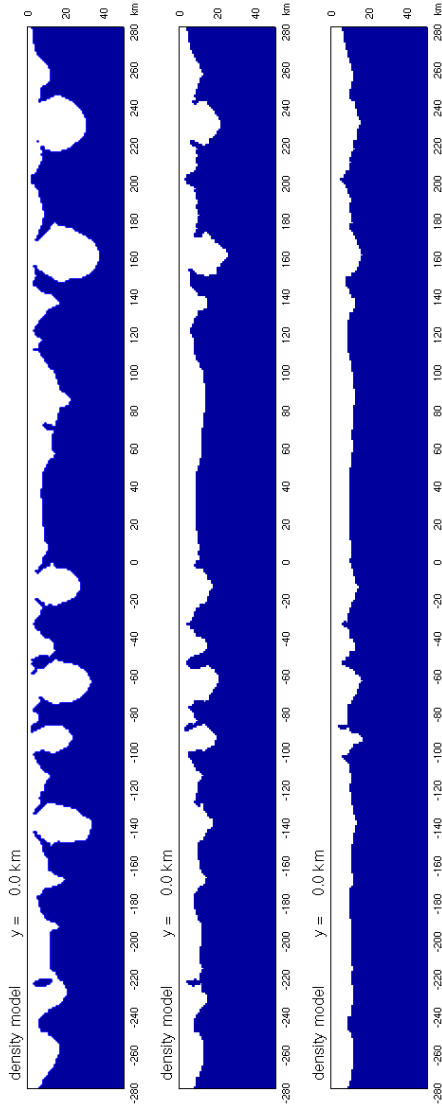


Fig. 9. Profile 8: density distribution in the vertical section 560×50 km along the profile for the original boundary depth 10 km for difference densities 100, 200 and 400 kg m^{-3} (top to bottom).

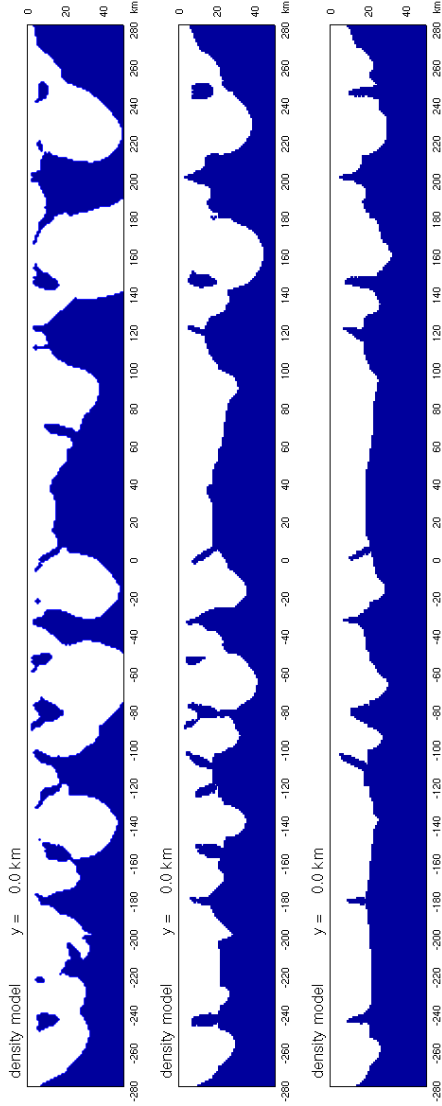


Fig. 10. Profile 8: density distribution in the vertical section 560×50 km along the profile for the original boundary depth 20 km for difference densities 100, 200 and 400 kg m^{-3} (top to bottom).

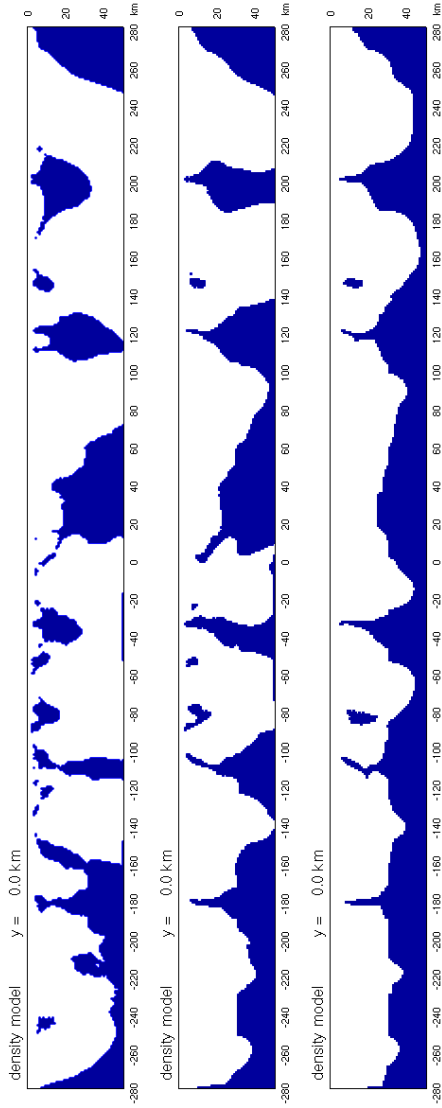


Fig. 11. Profile 8: density distribution in the vertical section 560×50 km along the profile for the original boundary depth 30 km for difference densities 100, 200 and 400 kg m^{-3} (top to bottom).

ity data, the difference between the two was at the order of 10 mGal at some parts of the studied profiles. Although declaring this as a fit is justifiable with respect to the error bars of the observed data, which themselves are quite substantial, still this difference, or misfit, constitutes too significant a signal which translates to a substantial uncertainty in terms of the determined structural density contrast interfaces at greater depths of the crust or the lithosphere. Without using additional geoscientific constraints, the purely gravimetric determination of these interfaces would be worse than poor. It is another task to assess how much can the constraining information diminish the uncertainty.

Acknowledgments. The authors were supported by VEGA grant agency under project No. 2/0107/09. Peter Vajda was partially supported by the Slovak Research and Development Agency under the contract No. APVV-0194-10.

References

- Dérerová J., Zeyen H., Bielik M., Salman K., 2006: Application of integrated geophysical modelling for determination of the continental lithospheric thermal structure in the Eastern Carpathians. *Tectonics*, **25**, 3, 1–12.
- Pohánka V., 2003: The harmonic inversion method: calculation of the multi-domain density. *Contrib. Geophys. Geod.*, **33**, 247–266.
- Pohánka V., 2003p: Testing of two variants of the harmonic inversion method on the territory of the eastern part of Slovakia. Power Point presentation and Video (zipped). <http://gpi.savba.sk/GPIweb/ogg/pohanka/pohanka.html>
- Pohánka V., 2004: Testing of the harmonic inversion method on the territory of the eastern part of Slovakia. *Österreichische Beiträge zu Meteorologie und Geophysik*, **31**, 190–190.
- Pohánka V., 2005: Universal interpolation method for many-dimensional spaces. Manuscript, 1–23. <http://gpi.savba.sk/GPIweb/ogg/pohanka/pohanka.html>
- Sandwell D. T., Smith W. H. F., 1997: Marine gravity anomalies from Geosat and ERS-1 satellite altimetry. *J. Geophys. Res.*, **102**, 10039–10054.
- Zeyen H., Fernández M., 1994: Integrated lithospheric modelling combining thermal, gravity and local isostasy analysis: application to the NE Spanish Geotranssect. *J. Geophys. Res.*, **99**, 18089–18102.
- Zeyen H., Dérerová J., Bielik M., 2002: Determination of the continental lithosphere thermal structure in the Western Carpathians: Integrated modelling of surface heat flow, gravity anomalies and topography. *Phys. Earth Planet. Inter.*, **134**, 89–104.